Control of pulse reverse electroplating parameters to enhance Cr diffusion barrier performance

SungSoo Ryu [a, b], JeongMok Oh [a], SungHwan Yeo [a], Sung Ho Kim [a], Young-Kook Lee [b], Jun Hwan Kim [a*]
[a]*Advanced Nuclear Fuel Development Division, Korea Atomic Energy Research Institute, Daedeok-daero 989-111, Yuseong-gu, Daejeon 34057, Republic of Korea*
[b]*Department of materials Science and Engineering, Yonsei University, Seoul 03722, Republic of Korea*
[*]*Corresponding author: junhkim@kaeri.re.kr*

Keywords : Diffusion barrier, Chromium coating, Electroplating, Pulse reverse currents, Fuel-cladding chemical interaction (FCCI), Sodium-cooled fast reactor (SFR), Cladding

1. Introduction

A Sodium-cooled fast reactors (SFR) is known for its ability to reduce radioactive waste by recycling used nuclear fuel from commercial reactors into metallic fuel through pyro-processing [1]. However, metallic fuel containing U, minor actinides, and fission products can chemically interact with the cladding (FCCI) [2]. The FCCI occurs above 650℃ and causes eutectics, which reduces the thickness of the cladding.

It is an imperative challenge to ensure the stability of metallic fuel. This study is using electroplating process to apply chromium (Cr) diffusion barrier coatings inside cladding tubes, aiming to mitigate FCCI. To evaluate the diffusion barrier property of Cr coatings, diffusion couple tests (FCCI test) were performed using the Ce-Nd (50:50 wt.%) alloy, which represent metallic fuel.

The electroplated Cr coatings formed by direct current (DC) or pulse current (PC) waveforms generate microcracks during electroplating process or FCCI test [3]. Microcracks serve as major diffusion pathways for Ce and Nd. For this reason, pulse reverse current (PR) waveforms were applied in this study to precisely control microcracks in the Cr coatings. Also, the diffusion resistance of PR electroplated Cr coatings (PR coatings) was evaluated by comparing the FCCI test results of DC and PC electroplated Cr coatings (DC and PC coatings).

2. Methods and Results

2.1 Cr Electroplating

During electroplating, the cathode-connected substrate was shaped into 12 mm diameter and 2 mm thickness disks using HT9, a material for cladding of nuclear metallic fuels. The disk surfaces were finally polished using a 3 um diamond suspension to minimize the influence of surface roughness during the Cr electroplating. Insoluble anodes, made of disk-shaped Pb-Sn alloy (9:1 wt.%), with a thickness of 2 mm were used. The plating solution was composed of deionized water, Cr trioxide, and H_2SO_4 in a ratio of 330:100:1. The plating bath temperature was maintained at 55 °C with a hotplate, and stirred at 150 rpm for uniform concentration distribution.

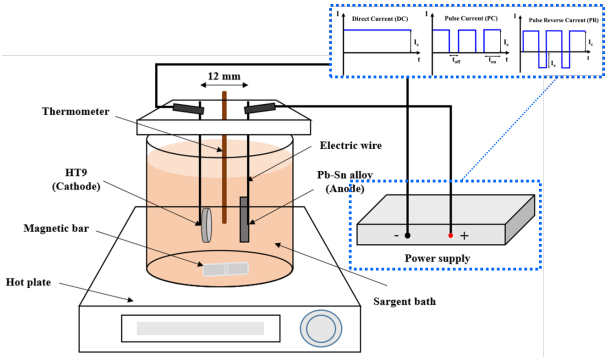

Fig. 1. Schematic of Cr electroplating devices.

2.2 PR process optimization

In contrast to electroplating by the DC and PC methods, the PR method effectively controls hydrogen, which induces residual stress, by applying anodic currents [4]. If the current density and time of anodic current (I_a and t_a) are not set appropriately, effective control of microcracks cannot be achieved. Therefore, it is essential to establish PR electroplating conditions via optimizing processes. Through a review of literature and experiments, this study established the optimal PR electroplating conditions by analyzing the impact of each parameter on the formation of PR coatings. The DC and PC electroplating conditions were set based on a previous study (Table I) [3].

Table I: Electroplating conditions of Cr coatings

Waveform	Cathode current density (A/cm^2)	Anode current density (A/cm^2)	Cathode time (msec/cycle)	Anode time (msec/cycle)	Plating time (min)	Temperature (℃)
DC	0.58	-	-	-		
PC	0.58	-	2000	2000	25-35	55
PR	0.58	0.16	9999	50		

2.3 4 FCCI test

The resistance of the Cr coating to FCCI was evaluated through diffusion couple tests (FCCI tests). The test alloy disks are representing nuclear fuel and consisting of Ce and Nd (50:50 wt.%). These disks were fabricated into disk shapes with a diameter of 8 mm and a thickness of 2 mm. Each Ce-Nd disk was aligned with

the Cr-coated HT9 surface and inserted into the testing jig for FCCI testing [5]. Subsequently, the specimen was heat-treated in a vacuum furnace at 650°C for 25 hours.

2.4 Microstructure analysis

The microcracks in the coating layers were observed using field emission scanning electron microscope (FE-SEM). Fig. 2 shows cross-sectional SEM images of as-coated specimens for each method. The DC coating showed numerous microcracks (Fig. 2(a)), while the PC or PR coating did not (Fig. 2(b) and 2(c)). In DC electroplating, microcracks form due to residual stress accumulation, while in the PC or PR electroplating, residual stress dissipates during off-time (t_{off}) or anodic time (t_a) intervals.

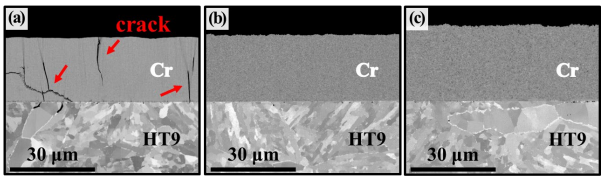

Fig. 2. Backscattered electron (BSE) microstructural observations in the cross-section of Cr electroplated using (a) DC, (b) PC, and (c) PR methods.

2.5 FCCI Resistance Evaluation

The microcracks and grain boundaries in coating layer serve as diffusion pathways for Ce/Nd. Diffusion of Ce/Nd predominantly occurs through microcracks in electroplated Cr coating. Subsequently, the diffused Ce/Nd interact with HT9, forming diffusion areas. Fig. 3 and 4 shows cross-sectional SEM images along with energy dispersive spectrometer (EDS) maps of FCCI tested specimens. For the DC electroplated Cr coating, diffusion occurred through relatively large microcracks, forming the large diffusion area (Fig. 3(a) and 4(a)). For the PC electroplated Cr coating, Ce/Nd diffusion progressed through cracks formed during the FCCI test (Fig. 3(b) and 4(b)). Microcracks in the PC coating arise from lattice distortion due to the phase transformation of hcp-CrH to bcc-Cr during heat treatment in FCCI testing [3]. Conversely, the PR electroplated Cr coating maintained stable, crack-free coating layers even at high temperatures. This is attributed to the periodic dissolution of hydrogen from chromium hydrides (CrH) in Cr coating layer, generated by appropriate anodic current, ultimately forming a coating composed of bcc-Cr. Consequently, no diffusion areas were observed in PR coating (Fig. 3(c) and 4(c)).

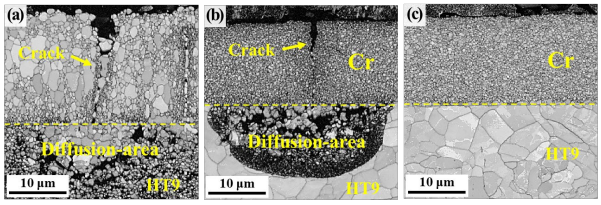

Fig. 3. SEM micrographs of FCCI-tested Cr-coated HT9 disk electroplated using (a) DC, (b) PC, and (c) PR methods.

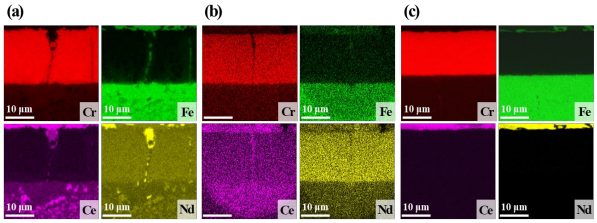

Fig. 4. EDS maps of FCCI-tested Cr-coated HT9 disk electroplated using (a) DC, (b) PC, and (c) PR method.

3. Conclusions

The critical factor in determining the FCCI resistance of electroplated Cr coatings is the presence of microcracks. For DC coating, FCCI resistance significantly decreases due to the formation of numerous cracks during electroplating. For PC coating, periodic t_{off} intervals alleviate residual stress, resulting in crack-free Cr coatings. However, during the 25-hour FCCI test at 650℃, meta-stable hcp-CrH in the PC coating layer transforms into bcc-Cr, leading to microcracks. On the other hand, the PR coating uses anodic currents to periodically relieve residual stresses and dissolve hydrogen in the CrH lattice, thereby forming crack-free Cr coatings composed of stable bcc-Cr. Consequently, the PR electroplated Cr coating maintained a stable diffusion barrier during the FCCI test, preventing the formation of microcracks and diffusion areas. This study introduced PR method to mitigate microcrack formation in electroplated Cr coatings. First, optimal conditions for the PR method were identified. Finally, through FCCI testing, the superior FCCI resistance of PR electroplated Cr coatings was confirmed compared to DC and PC coatings. The future research plan is to apply the PR method to the inner surface of cladding tubes (10-15 in length).

REFERENCES

[1] W. I. Ko, Preliminary conceptual design and cost estimation for SFR Fuel Manufacturing Facility (SFMF), Nuclear Engineering and Design, pp. 225-233, 2014.
[2] S. W. Yang, FCCI barrier performance of electroplated Cr for metallic fuel, Journal of Nuclear Material, pp. 98-103, 2010.

[3] S. H. Yeo, Direct and pulse electroplating effects on the diffusion barrier property of plasma-nitrided Cr coatings on HT9 steel, Journal of Nuclear Materials, pp. 154218, 2023.
[4] N. P. Wasekar, Influence of mode of electrodeposition, current density and saccharin on the microstructure and hardness of electrodeposited nanocrystalline nickel coatings, Surface & Coatings Technology, pp. 130-140, 2016.
[5] S. H. Yeo, The characterization of electrodeposited chromium barriers for nuclear reactor cladding application, Journal of Nuclear Materials, pp. 151980, 2020.